

Chapter 6

Laser-Assisted Electron Momentum Spectroscopy: Theory, Potential, and Perspectives

Konstantin Kouzakov

6.1 Introduction

My talk is devoted to laser-assisted electron momentum spectroscopy: its theory, potential, and perspectives. Here is an outline of my talk. In the first part, I will introduce you to the method of electron momentum spectroscopy and its theory. In the second part, I will speak about the electron momentum spectroscopy in the presence of the laser field, and particularly about the general theory of this method in the presence of the laser field. In the third part, I will present some recent numerical results for laser-assisted electron momentum spectroscopy of the helium atom, in particular, for ionization-excitation and double ionization. This case, i.e., the helium target, is important from the viewpoint of the experimental realization, which is expected in the near future. In the last part, I will briefly outline the potential and perspectives of the laser-assisted electron momentum spectroscopy.

6.2 Laser-Assisted Electron Momentum Spectroscopy

Let me introduce to you the method of electron momentum spectroscopy. This method is based on the $(e, 2e)$ process. The $(e, 2e)$ process means we have an incident electron that collides with the target A (see Fig. 6.1). The target can be an atom, molecule, cluster, or thin film. We have two electrons out, one is scattered and the other one is ejected. The key feature of electron momentum spectroscopy, if compared to the $(e, 2e)$ method in general, is that electron momentum spectroscopy investigates the kinematics of the so-called ‘quasielastic knockout’, that is, the

K. Kouzakov (✉)

Department of Nuclear Physics & Quantum Theory of Collisions, Faculty of Physics,
Lomonosov Moscow State University, Leninskie Gory 1, Moscow 119991, Russia
e-mail: kouzakov@gmail.com

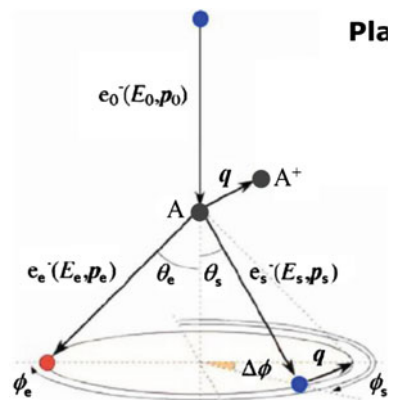
kinematics that is the closest to the free electron-electron collision. What does it give us? The point is that, under such kinematical conditions, the amplitude of the process is very well approximated within the plane-wave Born approximation, and the differential cross section is directly proportional to the momentum distribution of the electron in the so-called Kohn-Sham orbital. For this reason, it is often called the momentum profile. So, we measure the coincidence energies and momenta of the two final electrons and then, from the energy and momentum conservation laws, obtain the binding energy and momentum of the target electron. That is why it is called the electron momentum spectroscopy. The momentum of the target electron is opposite to the recoil-ion momentum \mathbf{q} and can be scanned by varying the out-of-plane azimuthal angle $\Delta\phi$.

Let me show how this method works. Figure 6.2 (borrowed from [1]) shows measured momentum profiles of atomic hydrogen versus theory. The theory is nothing else but an absolute square of the hydrogen wave function in momentum space.

The results of the more recent measurements from [2] are shown in Fig. 6.3. This case is not for hydrogen; this case is for helium. In the case of helium, in contrast to hydrogen, we do not know the exact wave function. Therefore, in the calculations, we use the different wave functions of helium. Thus we can select good wave functions and poor wave functions of helium (see Fig. 6.3). For example, here, 1 and 3 are poor wave functions.

Now, after introducing the basic principles of EMS, I pass to laser-assisted EMS. This part of my talk is based on the work of [3], where the idea of laser-assisted EMS was formulated and analyzed for the first time. Why laser-assisted EMS? The main reason is that it can be experimentally realized in the near future. The first laser-assisted ($e, 2e$) measurements have been already realized. However, they were conducted in the kinematical regime of small momentum transfer, which is very far from the kinematical regime of electron momentum spectroscopy. Currently, the first laser-assisted EMS measurements are in preparation, in Tohoku University (Sendai, Japan). The other important motivation is to examine the potential of the EMS method for studying the laser effects on momentum

Fig. 6.1 A schematic drawing of the ($e, 2e$) process for large momentum transfer



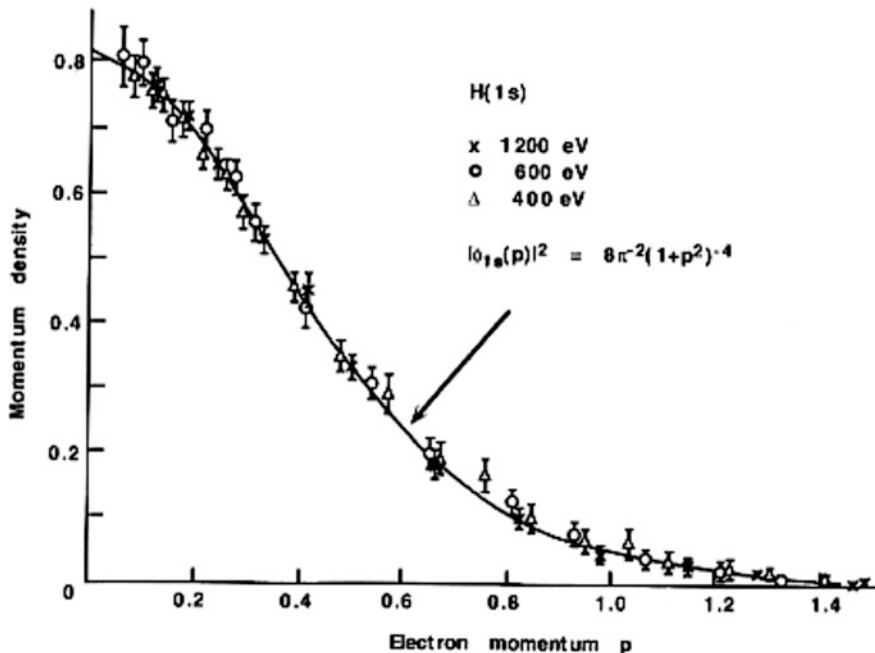


Fig. 6.2 The momentum profile for atomic hydrogen measured at the indicated energies compared with the square of the exact Schrödinger momentum-space wave function (solid line)

distributions of electrons in various systems, ranging from atoms and molecules to clusters and solids.

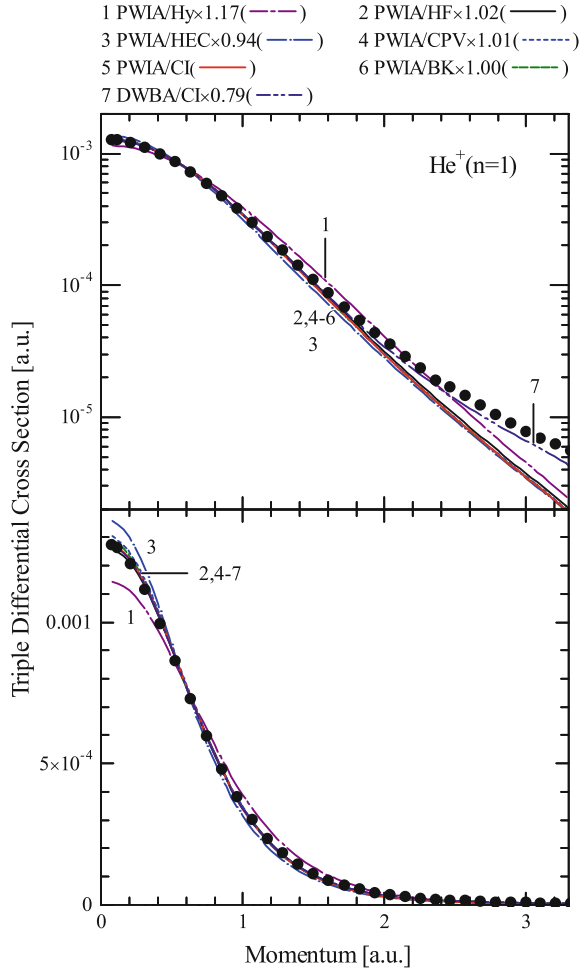
To analyze and interpret the data of such experiments, we need the proper theory. I will briefly present you the general theory of the laser-assisted electron momentum spectroscopy. I start with defining the laser field, so we assume that the laser field switches on and off adiabatically at $t \rightarrow \mp\infty$, respectively. The laser wavelengths are much greater than the spatial extent of both the target and the region where the electron-electron collision takes place, so this validates the use of the dipole approximation for the electric-field component of the laser field:

$$F(t) = F_0 \cos \omega t. \tag{6.1}$$

Another important condition is that the electric-field amplitude of the laser F_0 is much weaker than the typical electric field in the target F_T . This condition ensures that the laser field does not ionize the target before the (e, 2e) collision takes place.

The differential cross section, which is measured in the experiment, is derived from the S matrix. In the absence of the laser field, it is given by this formula:

Fig. 6.3 Comparison of experimental momentum profile of He for the transition to the $n = 1$ ground ion state with associated theoretical calculations using various variational wave functions



$$S = -2\pi i \langle \mathbf{p}_s \mathbf{p}_e | v_{ee} | \mathbf{p}_0 \psi_g \rangle \delta(E_0 + E_g - E_s - E_e), \quad (6.2)$$

where we have the electron-electron potential v_{ee} between two two-electron states. In the initial state, we have a plane wave for the incident electron and the ground-state wave function for the bound electron, ψ_g . In the final state, we have plane waves for the scattered and ejected electrons. The laser field modifies the plane waves into the Volkov functions, and so we end up with the Volkov-function Born approximation instead of the plane-wave Born approximation in the field-free case,

$$S = -i \int_{-\infty}^{\infty} dt \langle \chi_{\mathbf{p}_s}(t) \chi_{\mathbf{p}_e}(t) | v_{ee} | \chi_{\mathbf{p}_0}(t) \psi_T(t) \rangle. \quad (6.3)$$

Here the bound-electron state ψ_T is also modified by the laser field, so that it is a field-dressed target state.

The Volkov function is a solution to the Schrödinger equation, where we have the vector potential of the laser field. Without the vector potential the solution is a well-known plane wave. The Volkov function differs from the plane wave in phase. Namely, for the laser field that we are considering, it is given by the product of a usual plane wave, where the energy is shifted by a ponderomotive potential U_p , and the sum over the harmonics:

$$\chi_{\mathbf{p}}(\mathbf{r}, t) = \exp\{i[\mathbf{p} \cdot \mathbf{r} - Et - U_p t]\} \sum_{l,n=-\infty}^{\infty} e^{-i(l-2n)\omega t} J_l\left(\frac{\mathbf{p} \cdot \mathbf{F}_0}{\omega^2}\right) J_n\left(\frac{U_p}{2\omega}\right). \quad (6.4)$$

Here, J_l and J_n are Bessel functions of integer order.

The field-dressed target state solves the time-dependent Schrödinger equation, with the vector potential of the laser field and the target potential for the bound electron. The boundary condition

$$\psi_T(t \rightarrow -\infty) \rightarrow \exp(-iE_g t) \psi_g(\mathbf{r}) \quad (6.5)$$

means that, before the laser field switches on, we have the target electron in the ground state. According to the Floquet theorem, the solution can be presented in the form of the sum over the harmonics:

$$|\psi_T(t)\rangle = \exp(-i\tilde{E}_g t) \sum_{n=-\infty}^{\infty} e^{-in\omega t} |\psi_T^{(n)}(\tilde{E}_g)\rangle, \quad \tilde{E}_g = E_g + \Delta. \quad (6.6)$$

Here we have the quasi-energy \tilde{E}_g , which is shifted from the unperturbed energy E_g by the ac Stark shift. The ket-vectors $|\psi_T^{(n)}(\tilde{E}_g)\rangle$ are time-independent.

Thus, the fully differential cross section of the laser-assisted EMS process can be presented as a sum over the N -photon processes:

$$\frac{d^4\sigma}{dE_s dE_e d\Omega_s d\Omega_e} = \sum_{N=-\infty}^{\infty} d^3\sigma_N \delta(E_s + E_e - E_0 - \tilde{E}_g + U_p + N\omega). \quad (6.7)$$

If N is negative, it corresponds to the net absorption of N photons by the colliding system, and, if N is positive, to the net emission of N photons. The laser-assisted triple-differential cross section or the laser-assisted momentum profile is given by the following formula:

$$d^3\sigma_N = \frac{P_s P_e}{(2\pi)^3} \left(\frac{d\sigma}{d\Omega} \right)_{ee} |\psi_{T,N}(\mathbf{q})|^2, \quad \mathbf{q} = \mathbf{p}_s + \mathbf{p}_e - \mathbf{p}_0, \quad (6.8)$$

where we have the Mott electron-electron scattering cross section $\left(\frac{d\sigma}{d\Omega} \right)_{ee}$. The difference with respect to the field-free case is in the momentum profile:

$$\psi_{T,N}(\mathbf{q}) = \frac{\omega}{2\pi} \int_{-\pi/\omega}^{\pi/\omega} dt \exp \left\{ i \left(\tilde{E}_g - \frac{q^2}{2} - U_p - N\omega \right) t \right\} \langle \chi_{\mathbf{q}}(t) | \psi_T(t) \rangle. \quad (6.9)$$

Here we have a Volkov function instead of the plane wave. Let me recall that the momentum \mathbf{q} is opposite to the recoil-ion momentum and, in the EMS method, it is interpreted as a momentum of the bound electron before it is knocked-out by the incident electron. Having this general formula, we can obtain numerical results, and further I will present our recent numerical results for the case of the laser-assisted electron momentum spectroscopy of helium.

Why helium? As I already have mentioned, the first laser-assisted EMS measurements are in preparation. They are expected to be conducted on a helium atomic target. The expected laser parameters are as follows: the frequency is 1.55 eV, which is much lower than the excitation energy in helium; the intensity is such that the electric-field amplitude of the laser is much weaker than the typical electric field in helium.

The S matrix of the process is calculated from this formula:

$$S = -i \int_{-\infty}^{\infty} dt \langle \chi_{\mathbf{p}_s}(t) \chi_{\mathbf{p}_e}(t) \psi_f(t) | v_{ee} | \chi_{\mathbf{p}_0}(t) \psi_i(t) \rangle. \quad (6.10)$$

Here we have the Volkov functions for the incoming, $\chi_{\mathbf{p}_0}$, and outgoing electrons, $\chi_{\mathbf{p}_s}$ and $\chi_{\mathbf{p}_e}$, and the field-dressed states of the He atom, ψ_i , and the final He⁺ ion, ψ_f . v_{ee} is the electron-electron Coulomb potential. Since the laser electric field is weak, we can employ a perturbation theory for the field-dressed atomic and ionic states. This means that the main contribution to the field-dressed state comes from the field-free ground state, while the other field-free target states yield only small corrections.

To estimate first-order corrections to the field-dressed state of He and He⁺, we use the so-called closure approximation, where one replaces excitation energies in the systems with some respective average energies, called the closure parameters:

$$\psi_i(\mathbf{r}_1, \mathbf{r}_2, t) = e^{-i\varepsilon_{\text{He}} t} \left[1 - \frac{\mathbf{F}_0 \cdot (\mathbf{r}_1 + \mathbf{r}_2)}{\omega_{cl}} \cos \omega t \right] \Phi_i(\mathbf{r}_1, \mathbf{r}_2), \quad (6.11)$$

$$\psi_f(\mathbf{r}, t) = e^{-i\mathcal{E}_{1s}t} \left(1 - \frac{\mathbf{F}_0 \cdot \mathbf{r}}{\omega_{cl}} \cos \omega t \right) \varphi_{1s}(\mathbf{r}) \quad (6.12)$$

From these estimates of $\omega_{cl} \sim |\mathcal{E}_{\text{He}(1s)}|$, $\frac{F_0}{\omega_{cl}} \sim 10^{-3}$ a.u., it follows that the first-order corrections are negligible. Well, here we suppose that the He^+ ion after the ionizing collision remains in the state that corresponds to its unperturbed ground state, $n = 1$.

If the ion remains in the excited state, for example, in the first excited state, $n = 2$, then things become a little bit more complicated. Namely, now we must take into account the degeneracy of this state. We have $2s$ and $2p$ orbitals. Using this ansatz

$$|\psi_f(t)\rangle = \sum_{l=0,1} \sum_{m=-l}^l a_{lm}(t) e^{-i\mathcal{E}_{n=2}t} |2lm\rangle \quad (6.13)$$

when solving the time-dependent Schrödinger equation, we obtain the following results for the field-dressed states:

$$\begin{aligned} \psi_{2s}(\mathbf{r}, t) = e^{-i\mathcal{E}_{n=2}t} & \left[\cos\left(\frac{3F_0}{Z\omega} \sin \omega t\right) \varphi_{2s}(\mathbf{r}) \right. \\ & \left. - i \sin\left(\frac{3F_0}{Z\omega} \sin \omega t\right) \varphi_{2p_0}(\mathbf{r}) \right], \end{aligned} \quad (6.14)$$

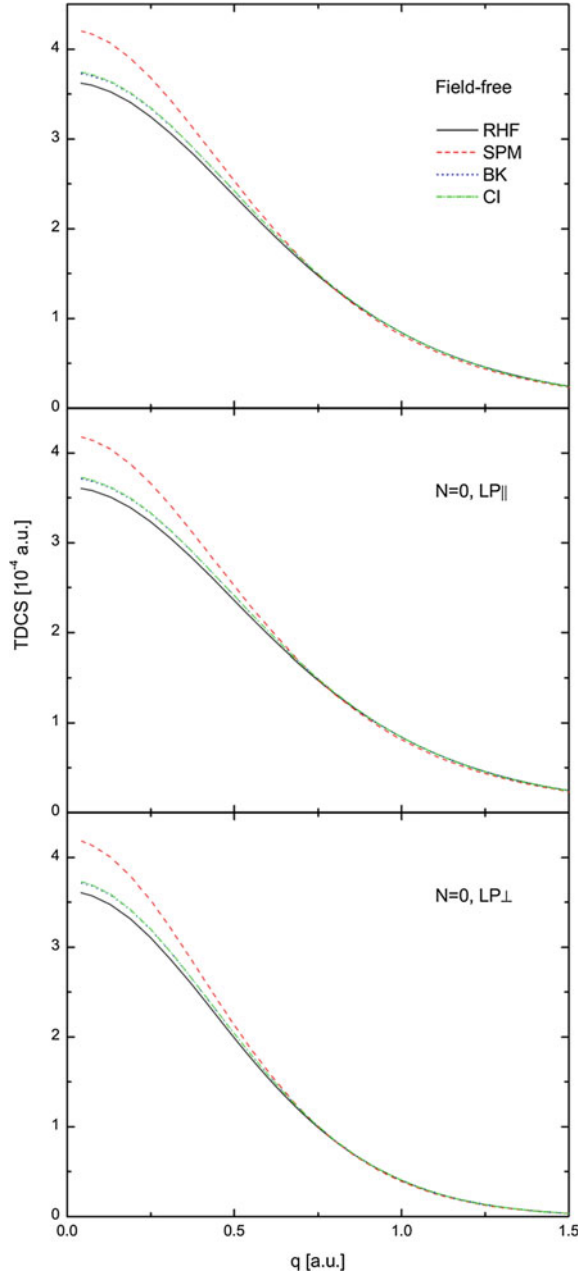
$$\begin{aligned} \psi_{2p_0}(\mathbf{r}, t) = e^{-i\mathcal{E}_{n=2}t} & \left[\cos\left(\frac{3F_0}{Z\omega} \sin \omega t\right) \varphi_{2p_0}(\mathbf{r}) \right. \\ & \left. - i \sin\left(\frac{3F_0}{Z\omega} \sin \omega t\right) \varphi_{2s}(\mathbf{r}) \right], \end{aligned} \quad (6.15)$$

$$\psi_{2p_{\pm 1}}(\mathbf{r}, t) = e^{-i\mathcal{E}_{n=2}t} \varphi_{2p_{\pm 1}}(\mathbf{r}). \quad (6.16)$$

Further, I will present some numerical results when the He^+ remains in the ground state and when it remains in the first excited state (see Fig. 6.4).

The top panel shows the field-free momentum profiles, that is, the usual EMS, in the absence of a laser field. Four different models of the helium ground-state wave functions are shown in Fig. 6.5. It is important that the two functions, BK and CI, which give accurate values for the helium binding energy and which are strongly correlated, are indistinguishable. The LP_{\parallel} and LP_{\perp} panels correspond to the presence of a laser field: the LP_{\parallel} to the geometry, where the laser field is almost perpendicular to the momentum \mathbf{q} ; and the LP_{\perp} to the geometry, where the laser field is nearly parallel to the momentum \mathbf{q} . So, it is difficult to find any difference between the cases of the absence and the presence of the field. What is most important here is that we do not see any difference between the results using the two accurate correlated functions, BK and CI.

Fig. 6.4 Field-free and $N = 0$ laser-assisted momentum profiles, when the He^+ ion is left in the $n = 1$ state



In Fig. 6.6, the He^+ ion remains in the ground state, but the total number of photons is different from zero. We find that the laser-assisted momentum profiles are markedly different in the inspected two geometries.

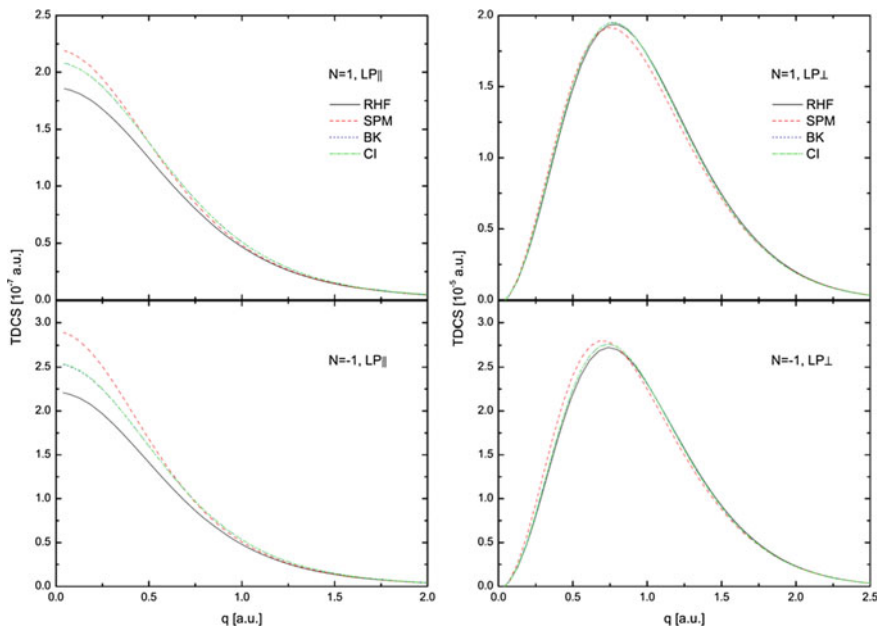


Fig. 6.5 The $N = \pm 1$ laser-assisted momentum profiles corresponding to the $(e, 2e)$ transition to the $n = 1$ state of He^+

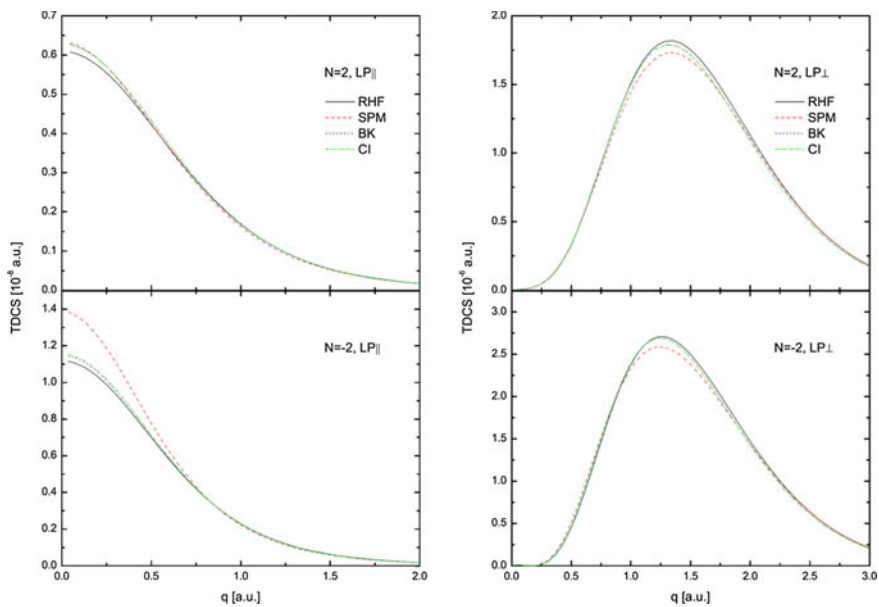
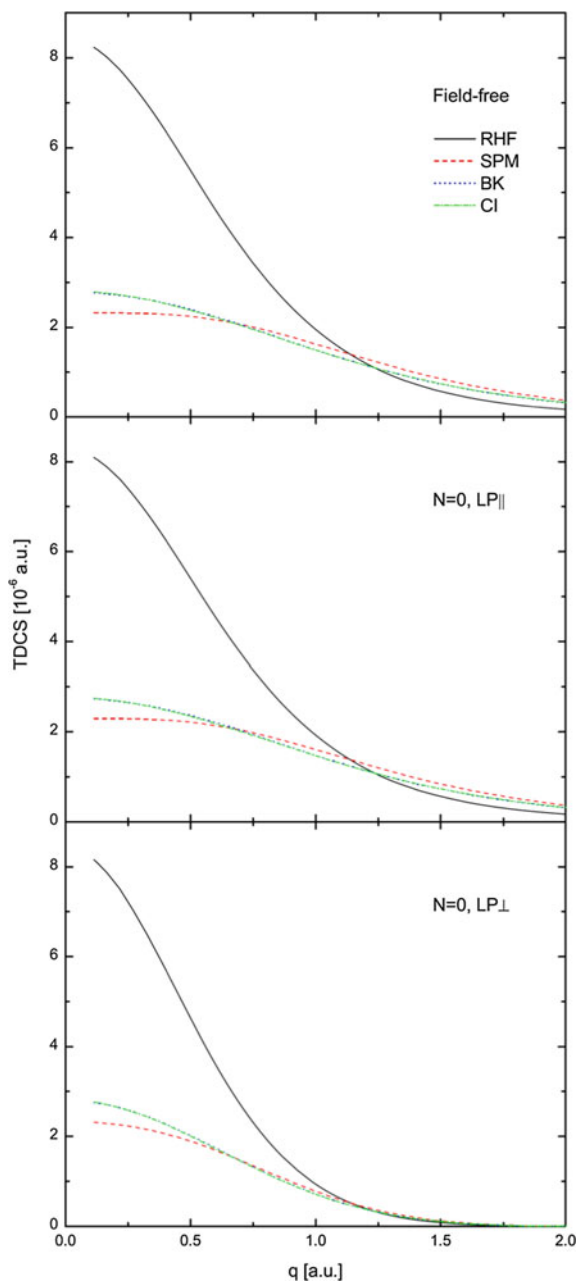


Fig. 6.6 The same as in Fig. 6.2, but for the $N = \pm 2$ case

Fig. 6.7 The same as in Fig. 6.4, but for the case when the He^+ ion is left in the $n = 2$ state



In this work [4], we showed that this difference is due to the effect of Volkov states on the fast incoming and outgoing electrons in EMS.

In Fig. 6.7, He^+ remains not in the ground but in the first excited state. The total number of photons is zero. The field-free and laser-assisted results. The same geometries exist, LP_{\parallel} and LP_{\perp} . Once again, no difference is found between the accurate functions, BK and CI.

However, if we consider the case of a nonzero number of photons, we can finally see the difference between the accurate functions (see Figs. 6.8 and 6.9).

This is a very important result, because, in EMS of helium in the absence of a laser field, you will never see any measurable difference between the accurate correlated functions (see Fig. 6.7).

Having obtained this finding, we decided to go further and to consider the situation when the He^+ is excited even higher, and as high as into the continuum. This is not the (e, 2e) case anymore, this is the so-called (e, 3e) case (see Fig. 6.10). We still have the fast incoming and two fast outgoing electrons, but, in addition, we measure a slow ejected electron simultaneously with the two fast final electrons.

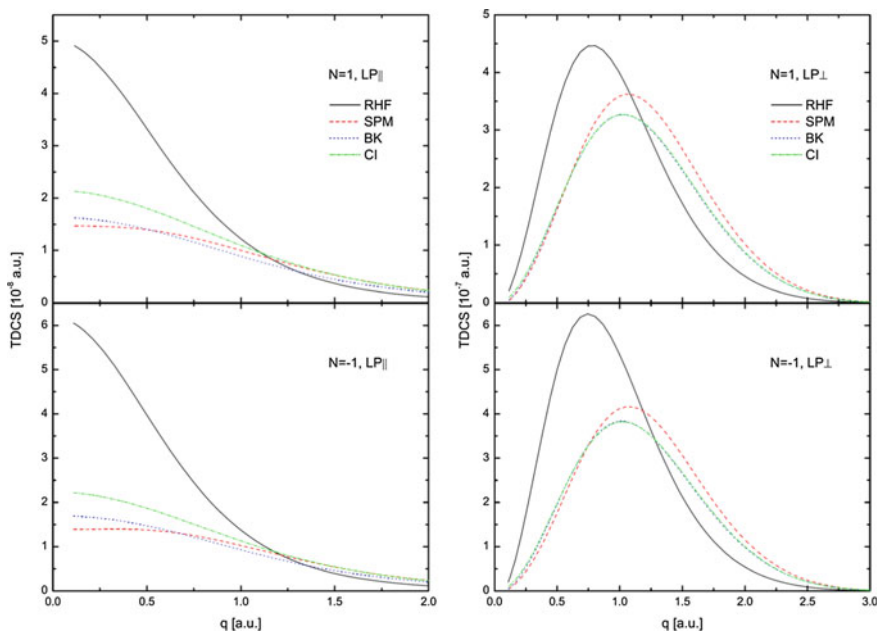


Fig. 6.8 The same as in Fig. 6.5, but for $n = 2$

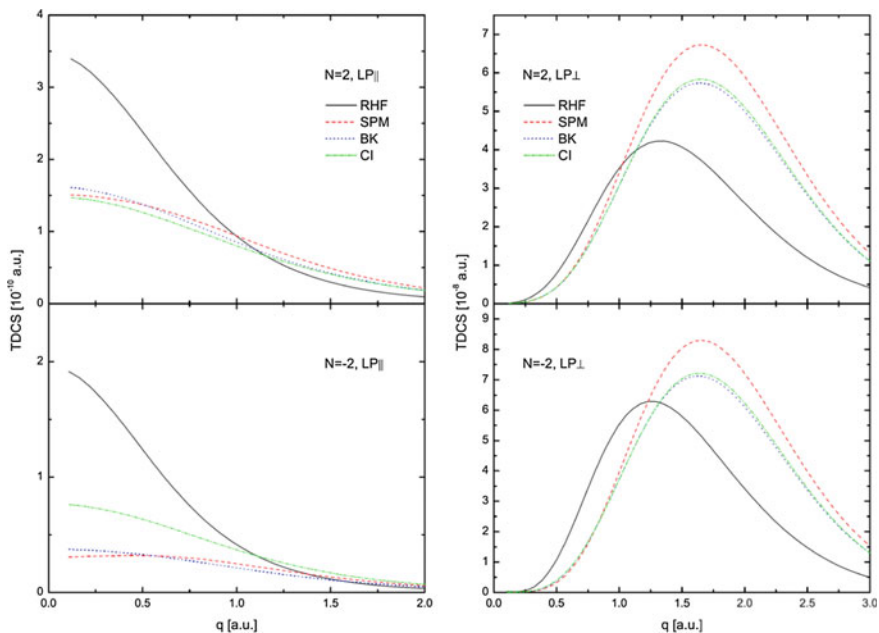
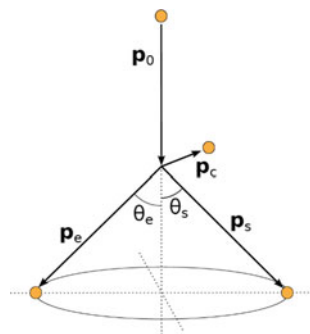


Fig. 6.9 The same as in Fig. 6.6, but for $n = 2$

Fig. 6.10 A schematic drawing of the $(e, 3e)$ process

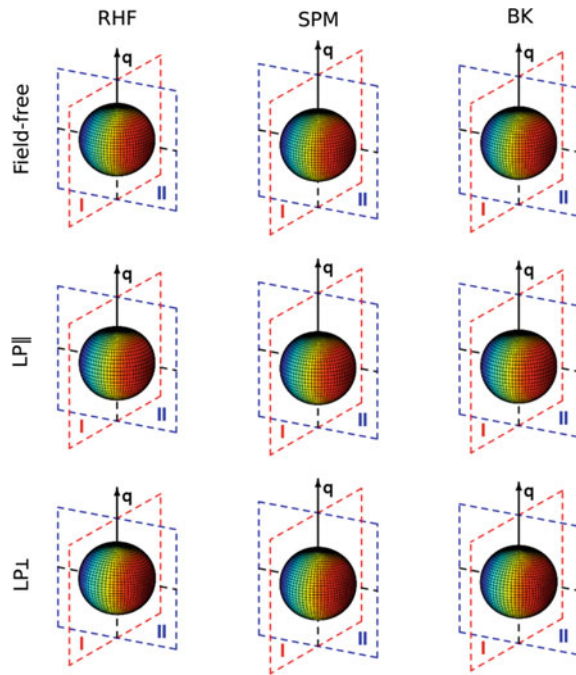


The slow ejected electron goes into the continuum due to the shake-off mechanism. The main problem here is how to describe this electron. We employed the so-called Coulomb-Volkov approximation:

$$\xi_{\vec{p}}^C(\vec{r}, t) = \varphi_{\vec{p}}^C(\vec{r}) \chi_{\vec{p}}(\vec{r}, t) \exp(-i\vec{p} \cdot \vec{r}). \quad (6.17)$$

Here the Coulomb wave takes into account the effect of the Coulomb field of the He nucleus on the slow electron, and the Volkov function takes into account the

Fig. 6.11 Numerical results for angular distributions of the slow ejected electron in the $(e, 3e)$ process. The scattering (*I*) and perpendicular (*II*) planes are indicated by the red and blue lines, respectively. The dashed line in plane *II* is perpendicular to the q axis and crosses the latter at the origin. The field-free angular distributions are shown in the *top row*, and the $N = 0$ results are shown in the *middle* (LP geometry) and *bottom* (LP $_{\perp}$ geometry) rows



effect of the laser field. Fig. 6.11 shows the results for the angular distributions of the slow electron when the momentum of the fast electrons are fixed.

The field-free and laser-assisted results with different functions of He are shown in Fig. 6.12. When the number of photons is zero, we find no difference. But when we consider a non-zero number of photons, we obtain marked differences between various different wave functions of He.

This means that the presence of the laser field strongly enhances the sensitivity of the EMS method to the electron-electron correlations.

What is interesting is that registering the slower electron is crucial to observe the difference between the different models of the He wave function. What is shown in Fig. 6.13 is the situation when the slow electron is not detected, the so-called $(e, 3-1e)$ case.

We find no difference between the field-free and laser-assisted results. Basically, when we do not register the slow ejected electron, we thus sum over different multiphoton processes. Since we consider a weak low-frequency field, we can use the Kroll-Watson sum rule that gives us the field-free result.

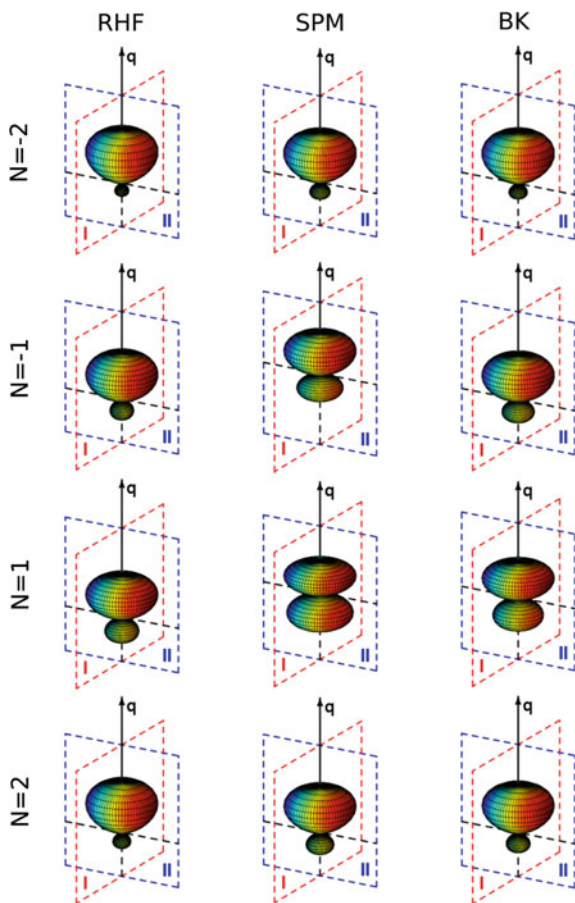


Fig. 6.12 The same as in Fig. 6.11, but for $N = -2, -1, 1, 2$ (from the *top* to the *bottom* row, respectively) in the LP_{\parallel} geometry

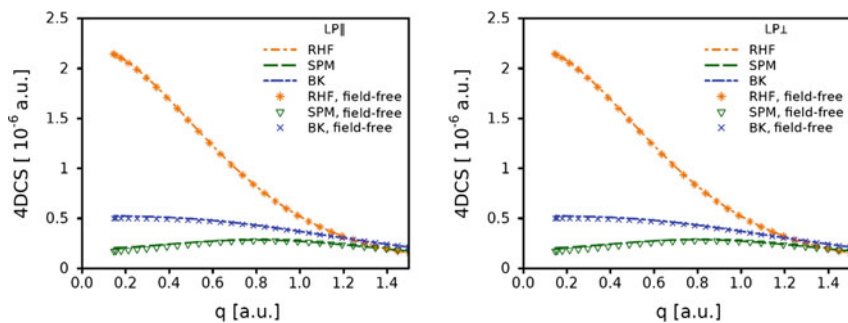


Fig. 6.13 The field-free and laser-assisted (e , 3-1e) momentum profiles in the (*left*) LP_{\parallel} and (*right*) LP_{\perp} geometries

6.3 Conclusion

Let me briefly outline potential and perspectives of the laser-assisted EMS method. Concerning the potential, our theoretical analysis for helium shows that even in the presence of the weak laser field, whose effect on the target state is almost insignificant, the sensitivity of the EMS method to electron-electron correlations in the target can be dramatically enhanced. Another interesting situation, which I did not discuss in my talk, is when the laser field is resonant with the transition in the target. In this case, even a very weak laser field can efficiently couple the ground and excited target states. One thus obtains a unique opportunity to study momentum distributions of electrons in excited states, because, in the absence of the laser field, you study only the ground state.

Finally, about perspectives: From the experimental side, we are waiting for the first laser-assisted measurements. These measurements are expected to be conducted on a helium atomic target with these laser parameters: $\omega = 1.55$ eV, $I = 5 \times 10^{11}$ W/cm². From the theoretical side, it will be interesting to consider the case of molecular targets. The other interesting development is the so-called time-resolved electron momentum spectroscopy. The idea is a pump-and-probe experiment, where the pump is a laser pulse and the probe is the electron pulse. Changing the time interval between the laser and electron pulses, one can create a kind of a movie in momentum space. This idea awaits a proper theoretical formulation.

References

1. E. Weigold, I.E. McCarthy, *Electron Momentum Spectroscopy* (Kluwer Academic/Plenum Publishers, New York, 1999)
2. N. Watanabe et al., *Phys. Rev. A* **72**, 032705 (2005)
3. K.A. Kouzakov, Yu.V. Popov, M. Takahashi, Laser-assisted electron momentum spectroscopy, *Phys. Rev. A* **82**, 023410 (2010)
4. A.A. Bulychev, K.A. Kouzakov, Yu.V. Popov, The role of Volkov waves in laser-assisted electron momentum spectroscopy. *Phys. Lett. A*. **376**, 484–487 (2012)